INTERNATIONAL JOURNAL OF ELECTRICAL AND POWER ENGINEERING

MEDWELL PUBLICATIONS

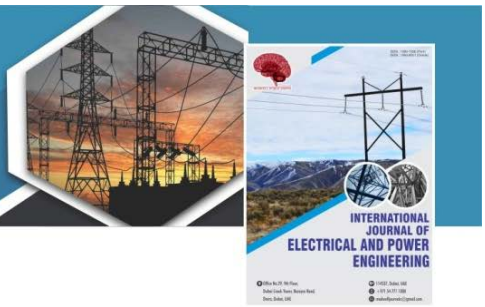

# Comparison Between Multi-Break Circuit Breaker and Cascaded Series Circuit Breakers

Mahmoud Ahmed Saad
*Department of Power and Electrical, Benha Faculty of Engineering, Benha University, Tukh, Egypt*

**Key words:** HVDC circuit breaker, cassie breaker, modifications, arc, voltage

**Corresponding Author:**
Mahmoud Ahmed Saad
*Department of Power and Electrical, Benha Faculty of Engineering, Benha University, Tukh, Egypt*

Page No.: 68-84
Volume: 14, Issue 6, 2020
ISSN: 1990-7958
International Journal of Electrical and Power Engineering


**Abstract:** Arc interruption of High Voltage Direct Current (HVDC) Circuit Breakers (CBs) is one of the main challenging factors for using HVDC grids. To evaluate the arc interrupting capability in HVDC circuit breakers, black box arc models are used to represent the non-linear arc conductance depending on Cassie and Mayrdynamic arc equations. A real line represents a part of 500 kV electrical connection systems between Egypt and Kingdom Saudi Arabia is simulated to be a faulty load. It is found that the arcing voltage and thearcing time of the HVDC CB can be reduced by decreasing the value of arcing time constant( ) and increasing the value of power cooling coefficient (P) It is also deduced that the arcing time is reduced by the increase of the commutation capacitance value (C) and decreasing the commutation inductance (L) value and vice versa. Moreover, it is concluded that the arcing voltage of HVDC circuit Breaker is greatly affected if more than one pole (cascaded series or parallel two or three poles) are used for single circuit breaker and this would be more effective and better for commercial reasons than using cascaded series or parallel two or three circuit breakers.

## INTRODUCTION

In September, 2020, High Voltage Direct Current (HVDC) Circuit Breakers (CBs) play a vital role in the growth of HVDC power systems which can widely help in replacing fossil fuels with renewable energy sources[1-8]. The main usage of HVDC system is to connect two AC networks with different frequencies and to transmit large amounts of power via. long distances[9-16].

The key challenge that faces the expansion of HVDC CBs is the absence of natural current zero crossing. As a matter of fact, in AC interrupting processes the current decrease to zero naturally. On the other hand, in DC interrupting processes the current needs to be forced to zero. Therefore, to form a HVDC CB, it is necessary to install additional components on conventional AC circuit breaker to form artificial current zero crossing[16-19]. A lot of works have been directed to create artificial zero crossing in the DC current by using active and passive commutation types[19, 19-21].

Arc is considered the main aspect of the interruption process. Many electric arc models are developed for describing arc behavior[16, 21-24]. Conventional arc models are classified into physical arc models and black box arc models. The physical arc model describes the entire arc behavior during the interruption. Therefore, it can be used to investigate the arc behavior in details but it is very complicated to be applied. Otherwise, the black box arc

model can be considered the proper method to describe the arc behavior[16, 25-28]. Black box models represent the non-linear arc conductance variation with time[16, 21-25]. The choice of black box model equations to determine their parameters is essential, hence, it requires making certain assumptions about the arc behavior[16, 17-20].

As the main purpose of the black box arc model is to describe the interaction between the arc and the electrical circuit during the current interruption process, cassie and Mayr dynamic arc equations can be considered the most representative arc models[16, 17-19].

For applying Mayr's model to interrupt DC current, a resonance (LC) circuit is coupled in parallel with the circuit breaker to generate self-excited oscillatory current superimposed on the DC current forming zero current crossing[16, 17, 22-35]. However, when applying Cassie's model, there is no need to use a parallel resonance circuit with the breaker, it is only required to make the steady state arc voltage over supply voltage to decrease the current quickly to zero[16, 21]. Besides, a circuit element is used to control the Rate of Rise of Recovery Voltage (RRRV) and an absorber element to absorb the energy stored in the system inductance after arc interruption. These two circuit elements are used with the arc simulation by both Mayr and Cassie models[16, 19, 33].

This study makes a comparison between multi-break circuit breaker and cascaded series circuit breakers like: multi-break consisting of 2 contacts in comparison with 2 series circuit breakers and multi-break consisting of 3 contacts in comparison with 3 series circuit breakers DC fault test bed modeling is carried out by MATLAB/Simulink software to evaluate the capability to protect the HVDC overhead transmission line, connecting Badr substation in Egypt and Elnabaq switching station. Such line represents a part of 500 kV electrical connection systems between Egypt and Kingdom Saudi Arabia.

## MATERIALS AND METHODS

**Modeling of HVDC circuit breaker:** Figure 1 shows the puffer type of SF6 gas CB structure including the simulated arc, rated voltage of 525 kV, lightning impulse withstand voltage of 1175 kV, rated normal current of 2000 A, rated short time current (1s) of 40 kA, rated peak withstand current of 100 kA and rated short circuit making current of 100 kA.

As it is known, the HVDC arc can be considered as a nonlinear phenomenon which occurs due to two factors. The first one is the high short circuit current that generates heat leading to the circuit breaker contacts and quenching medium temperatures increase, consequently a sufficient quantity of electrons are emitted. In addition, at the arc initiation when the value of the voltage between the two contacts exceeds the ionization voltage of the inter-electrode gas, the gas may be sufficiently ionized.

SF6 gas has electro-negativity characteristics which means that the SF6 gas takes the free electrons far away from the field as a result of this action; the SF6 gas becomes electrically unstable and leaves the electrons quickly. Consequently, the electrons move in a random motion where the only way to reignite the arc is to achieve an oriented motion of the free electrons. Black box arc models are applied using the models of Mayr and Cassie. Mayr's equation can be deduced from the energy balance equation as given in Eq. 1:

$$dQ/dt = (H)-P(Q) \quad (1)$$

where, P(H) is the heat generated with the assumption that the cooling power P(Q) and the arc conductance g(Q) are arbitrary functions of Q. The general form of the dynamic arc equation of current i is represented as follows:

$$dg/dt = (1/[dQ/dg]*(i^2/g-p) \quad (2)$$

By further assumption of Q = Q0. ln (g/G0) where Q0 and G0 are constants describing the arc, the thermal time constant is defined by = Q0/p. Thus, Mayr dynamic arc equation can be presented as given in Eq. 3:

$$(P*\tau/g)*dg/dt = i^2/g-p \quad (3)$$

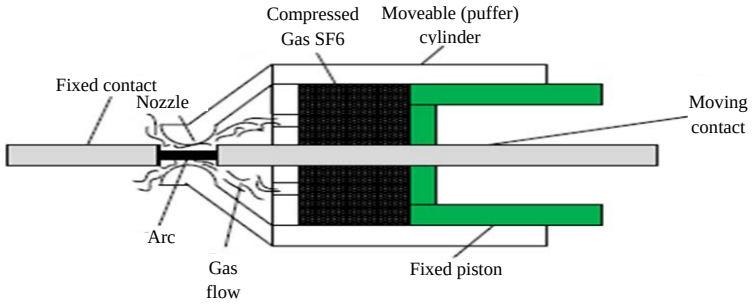


Fig. 1: The puffer type of SF6 circuit breaker structure

It is worth mentioning that by eliminating the hypothesis has the time constant and cooling power p are constants, it leads to a generalized form of Mayr's equation as given below in Eq. 4 where u is the arc voltage:

$$(1/g)*dg/dt = 1/\tau(u^2/Uc^2-1) \quad (4)$$

Meanwhile, cassie defines the arc behavior with the following hypothesis and assumptions: the arc column has a cylindrical shape filled with highly ionized gas and free electrons, arc cylindrical column has uniform temperature and current density but its diameter is altered in time and accommodate the change in current, arc voltage is considered constant during the arc process and finally, the power dissipation is considered proportional to the column cross sectional area. With these assumptions, a linear relation between arc conductance and energy storage capacity of the arc is presented by the following Eq. 5 which represents the last form of Cassie's equation:

$$(1/g)*dg/dt = 1/\tau(u^2/Uc^2-1) \quad (5)$$

Where:

$\tau$ = The arc time constant
p = The arc power loss coefficient
g = The arc conductance (i/u)
u = The arc voltage
Uc = The steady state arc voltage

After simulating the non-linear arc conductance using black box arc models, it should be noted that there is a need to use additional circuit elements that connected with HVDC CB to interrupt the electrical arc[16].

## RESULTS AND DISCUSSION

Figure 2-9 illustrate the results of using two series cascaded circuit breakers. It is noticed that when the DC current reaches toapproximately 20 kA, the fault is detected and the DC circuit breaker successfully starts to open at 0.01 sec and the electrical arc isgenerated as it is observed in Fig. 4 and 5.

It is also noticed that from Fig. 5 at the point of 0.01118 sec, the HVDC CB completely interrupts the arc current andextinguishes the arc. As the max peak of voltage value across CB in thissystem is 385 kV as shown in Fig. 4, it is noticed from Fig. 6 and 7 that the fault is cleared after the energyabsorber element has absorbed the energy stored in thesystem inductance andthe current ceases to almost zero. Hence, we can notice that decreasing the value of inductance and increasing the value of capacitance helped in reducing the value of both arcing time and voltage. Moreover, using two series cascaded circuit breakers has decreased the voltage on each one of them. Also, the arcing time in this modification model has decreased. Note that the max peak of voltage across the two CBs is 770 KV. Figure 8 and 9 illustrate the results of changing the values of and P (Table 1).

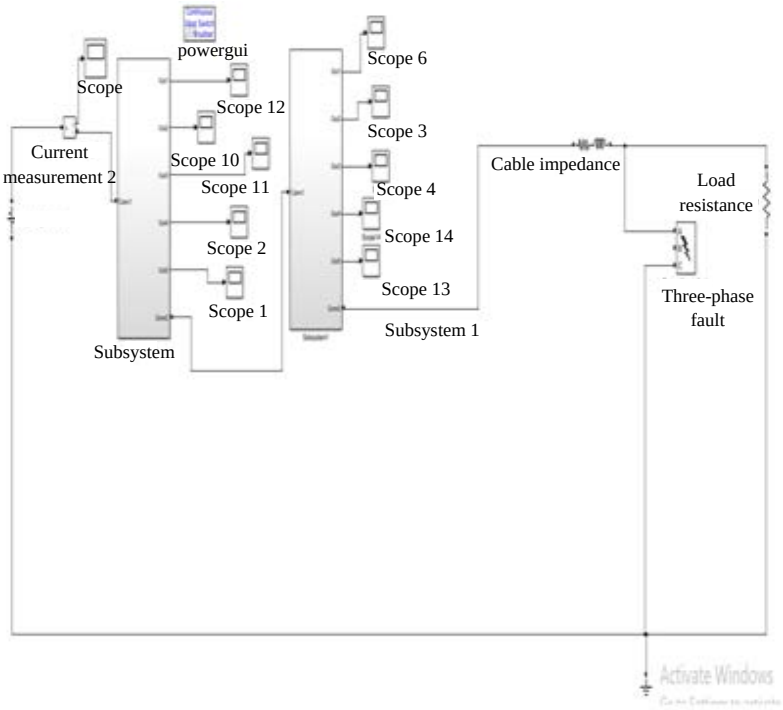


Fig. 2: The model of two series circuit breakers of Mayr model

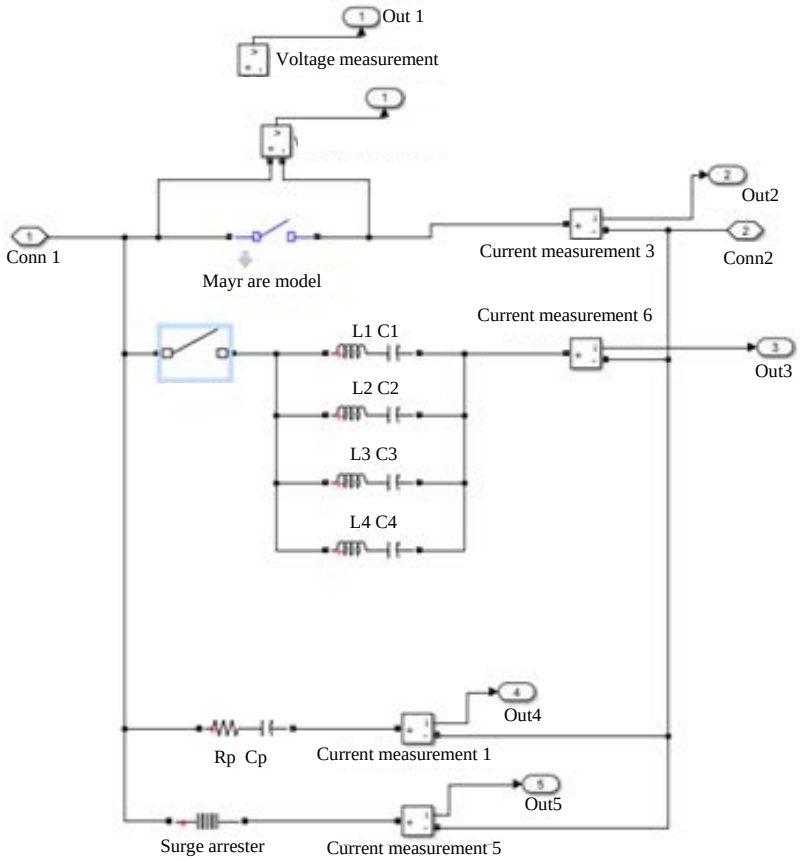


Fig. 3: The subsystem of each circuit breaker of the two series circuit breakers

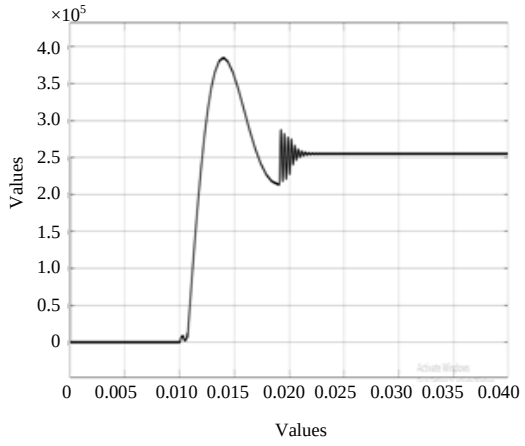


Fig. 4: The voltage across each circuit breaker

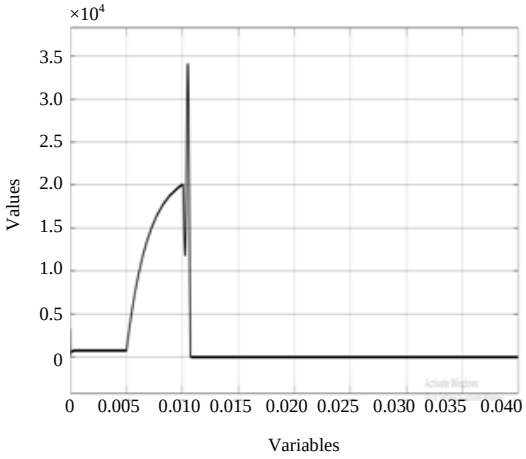


Fig. 5: The current through each circuit breaker

Figure 10-18 illustrate the results of using two series cascaded poles for one circuit breaker in the same tested Mayr model of circuit breaker to decrease the arcing time and voltage. It is noticed that when the DC current reaches to approximately 20 kA, the fault is detected and the DC circuit breaker successfully starts to open at 0.01 sec and the electrical arc is generated as it is observed in Fig. 12-14. It is also noticed that from Fig. 14 at the point of 0.01085 sec, the HVDC CB completely interrupts the arc current and extinguishes the arc. As the max peak of voltage value across CB in this system is 673.5 kV as shown in Fig. 12, it is noticed from Fig. 15

Table 1: Simulation parameters of the models of Mayr after using two series circuit breakers

| Model | Parameters | Default values | Tested values |
|---|---|---|---|
| Mayr | P (MW) | 100 | 65, 85, 115 |
| | ϑ (μ sec) | 10 | 5, 15, 20 |
| | L1-L4 (mH) | 0.25 | 0.25 |
| | C1-C4 (μF) | 20 | 20 |
| | Rp (Ω) | 75 | 75 |
| | Cp (μF) | 0.1 | 0.1 |

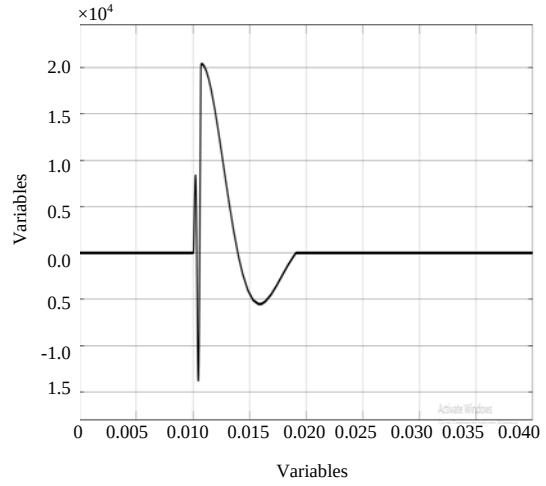


Fig. 6: The current through commutation circuit for each circuit breaker

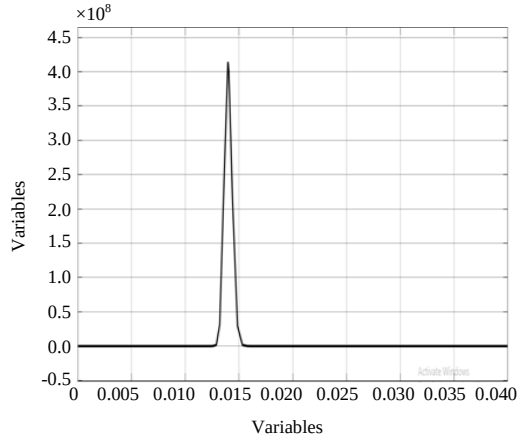


Fig. 7: The current through surge arrester for each circuit breaker

and 16 that the fault is cleared after the energy absorber element has absorbed the energy stored in the system inductance and the current ceases to almost zero. Hence, we can notice that decreasing the value of inductance and increasing the value of capacitance helped in reducing the value of both arcing time and voltage. Moreover, using two series cascaded poles for one circuit breakers has decreased the voltage on each pole of the CB as shown in

Table 2: Simulation parameters of the models of Mayr after using two series poles of each circuit breaker

| Model | Parameters | Default values | Tested values |
|---|---|---|---|
| Mayr | P (MW) | 100 | 65, 85, 115 |
| | ϑ (μs) | 10 | 5, 15, 20 |
| | L1, L2 (mH) | 0.25 | 0.25 |
| | C1, C2(μF) | 20 | 20 |
| | Rp (Ω) | 75 | 75 |
| | Cp (μF) | 0.1 | 0.1 |
| | R1, R2 (Ω) | 5 | 5 |
| | C5, C4 (pF) | 100 | 100 |

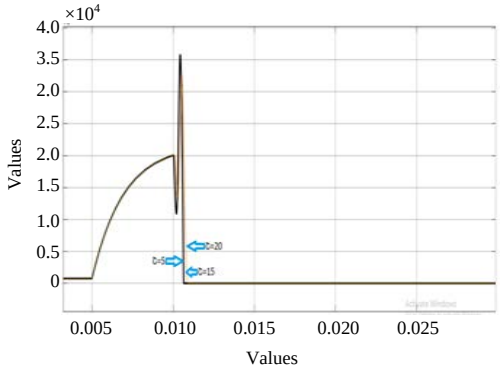


Fig. 8: The current through circuit breaker with various values of ϑ

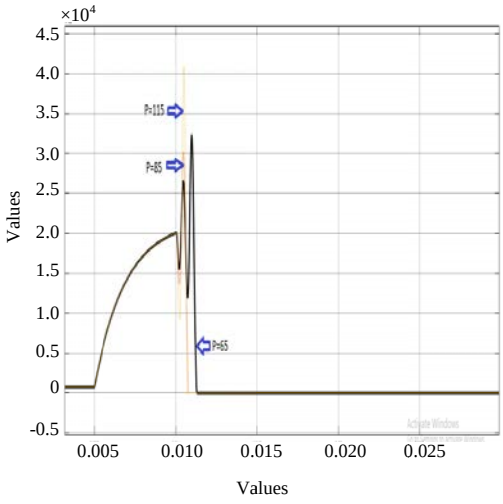


Fig. 9: The current through circuit breaker with various values of P

Fig. 13 and the total voltage on the CB. Also, the arcing time in this modification model is smaller than the past one (Table 2). Figure 17 and 18 illustrate the results of changing the values of P and ϑ .

Figure 19-26 illustrate the results of using three series cascaded circuit breakers in the same tested Mayr model of circuit breaker to decrease the arcing time and voltage. It is noticed that when the DC current reaches to approximately 20 kA, the fault is detected and the DC circuit breaker successfully starts to open at 0.01 sec and

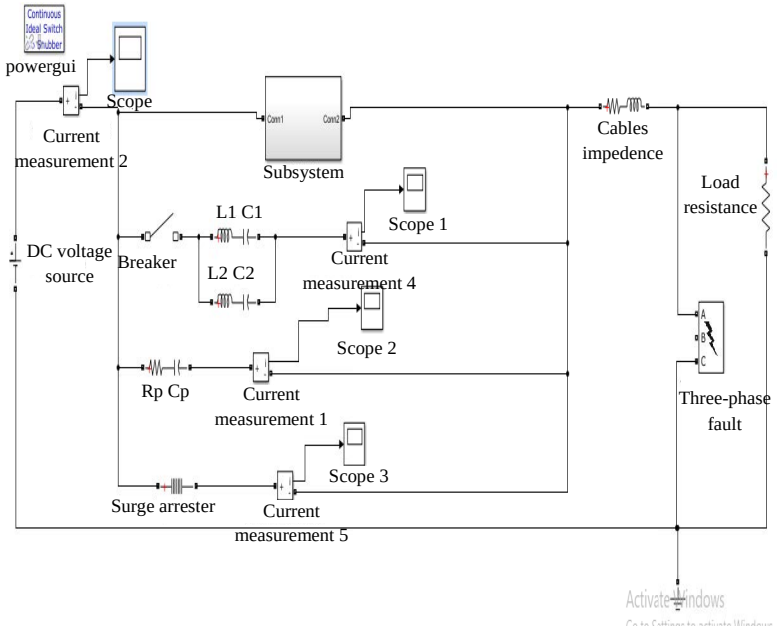


Fig. 10: The main model of circuit breaker consists of two poles

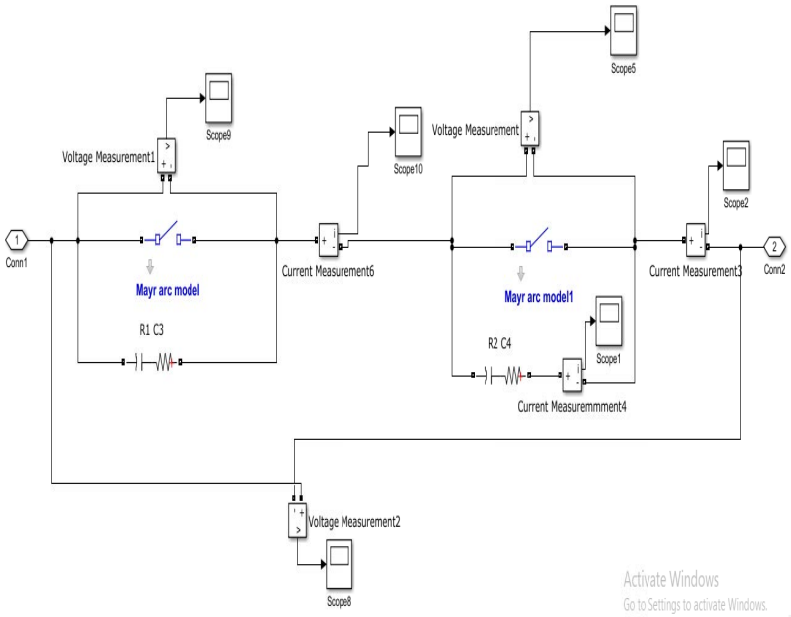


Fig. 11: The subsystem of the circuit breaker

the electrical arc is generated as it is observed in Fig. 21 and 22. It is also noticed that from Fig. 22 at the point of 0.01141 sec, the HVDC CB completely interrupts the arc current and extinguishes the arc. As the max peak of voltage value across CB in this system is 300 kV as shown in Fig. 21, it is noticed from Fig. 23 and 24 that the fault is cleared after the energy absorber element has absorbed the energy stored in the system inductance and the current ceases to almost zero. Hence, we can notice that decreasing the value of inductance and increasing the value of capacitance helped in reducing the value of both arcing time and voltage. Moreover, using two series cascaded circuit breakers has increased the total voltage on the three CBs but has decreased the voltage on each one of them than the regular one. Also, the arcing time in this modification model is greater than the past one (Table 3). Figure 25 and 26 illustrate the results of changing the values of P and .

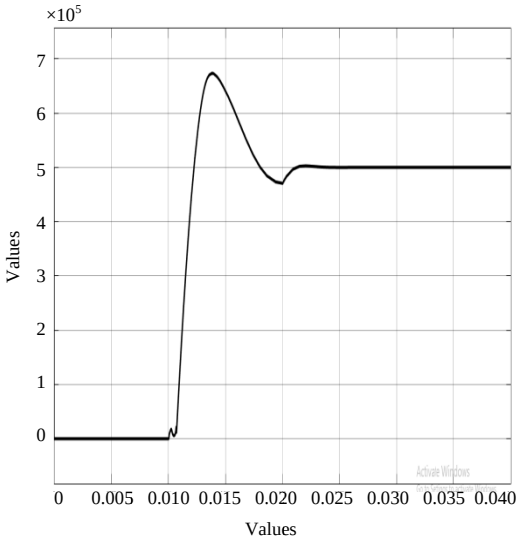


Fig. 12: The total voltage across the circuit breaker

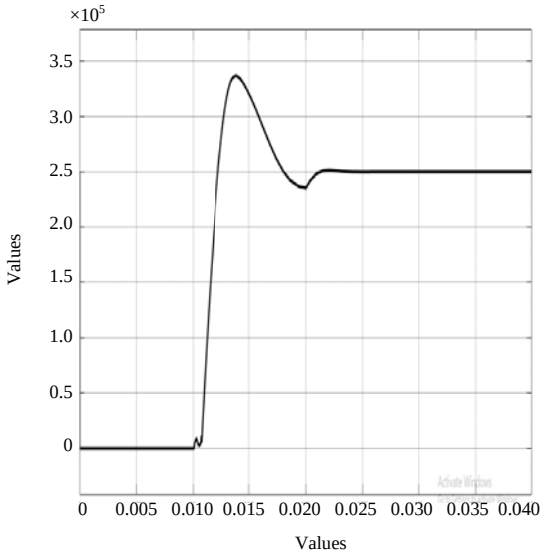


Fig. 13: The voltage across each pole of the circuit breaker

Table 3: Simulation parameters of the models of Mayr after using three series circuit breakers

| Model | Parameters | Default values | Tested values |
|---|---|---|---|
| Mayr | P (MW) | 100 | 65, 85, 115 |
| | ὸ (μs) | 10 | 5, 15, 20 |
| | L1-L4 (mH) | 0.25 | 0.25 |
| | C1-C4 (μF) | 20 | 20 |
| | Rp (Ω) | 75 | 75 |
| | Cp (μF) | 0.1 | 0.1 |

Figure 27-35 illustrate the results of using three series cascaded poles for one circuit breaker in the same tested Mayr model of circuit breaker to decrease the arcing time and voltage. It is noticed that when the DC current

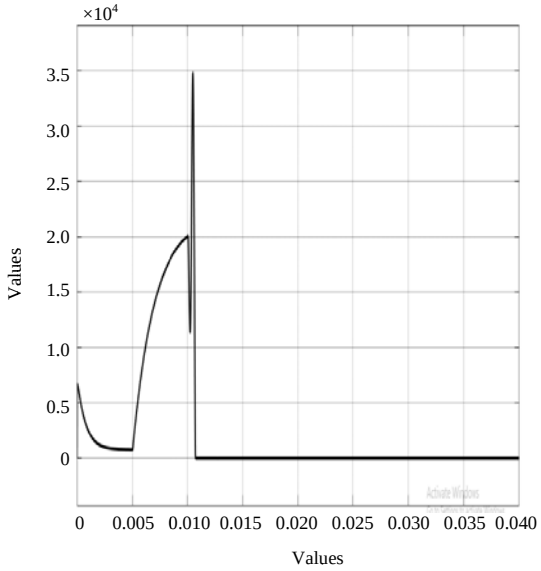


Fig. 14: The current through the circuit breaker

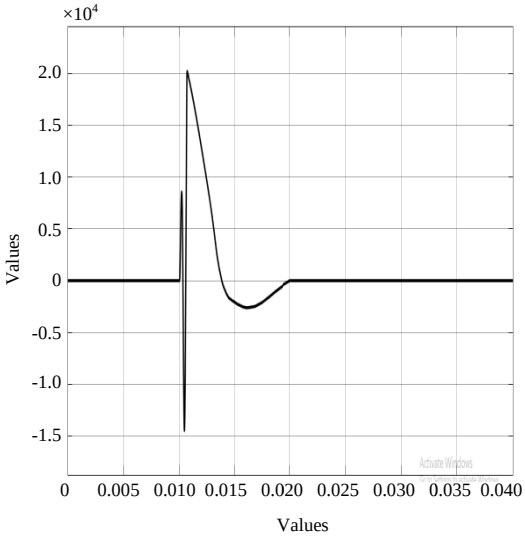


Fig. 15: The current through the commutation circuit

reaches to approximately 20 kA, the fault is detected and the DC circuit breaker successfully starts to open at 0.01 sec and the electrical arc is generated as it is observed in Fig. 29 and 31 (Table 4).

It is also noticed that from Fig. 31 at the point of 0.01228 sec, the HVDC CB completely interrupts the arc current and extinguishes the arc. As the max peak of voltage value across CB in this system is 654 kV as shown in Fig. 29, it is noticed from Fig. 32 and 33 that the fault is cleared after the energy absorber element has absorbed the energy stored in the system inductance and the current ceases to almost zero. Hence, we can notice that decreasing the value of inductance and increasing the value of capacitance helped in reducing the value of both

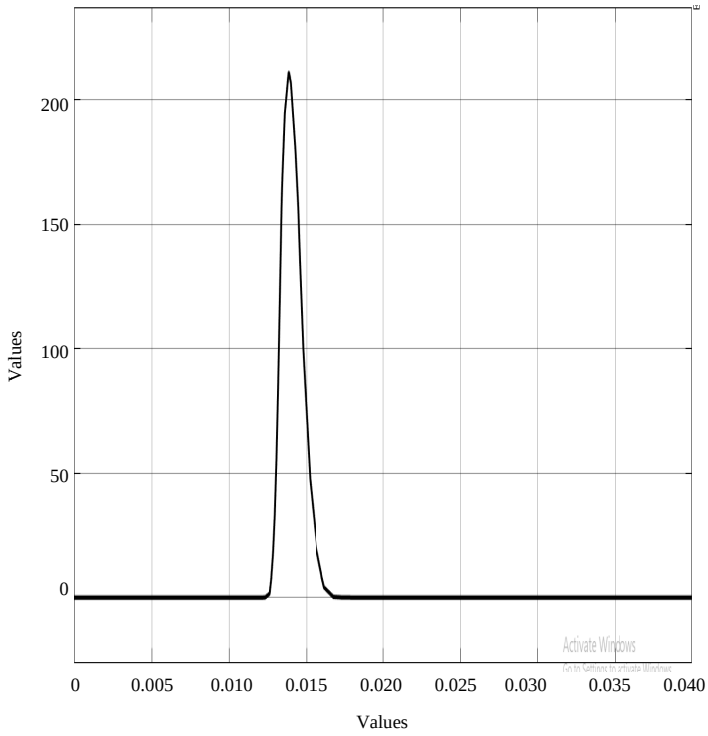


Fig. 16: The current through the surge arrester

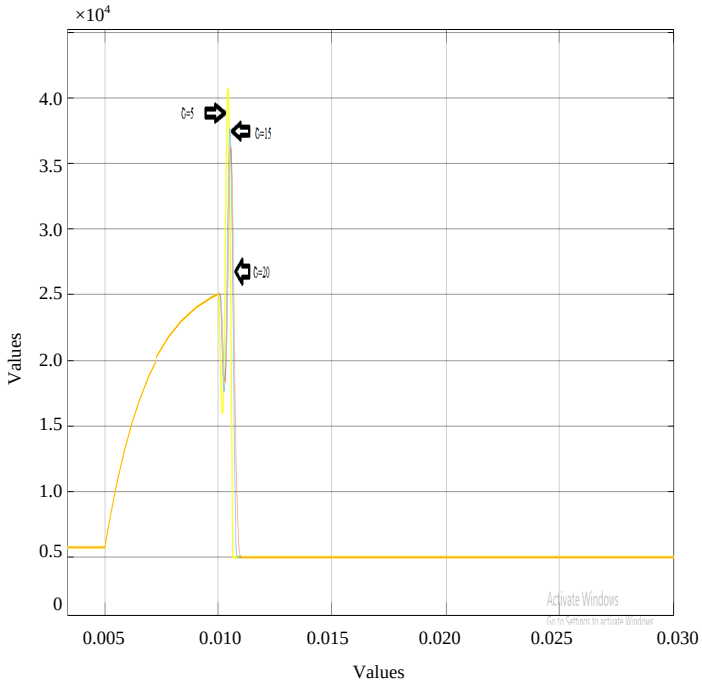


Fig. 17: The current through circuit breaker with various values of ϑ

arcing time and voltage. Moreover, using three series cascaded poles for one circuit breakers has decreased the voltage on each pole of the CB as shown in Fig. 30 and the total voltage on the CB. Also, the arcing time in this

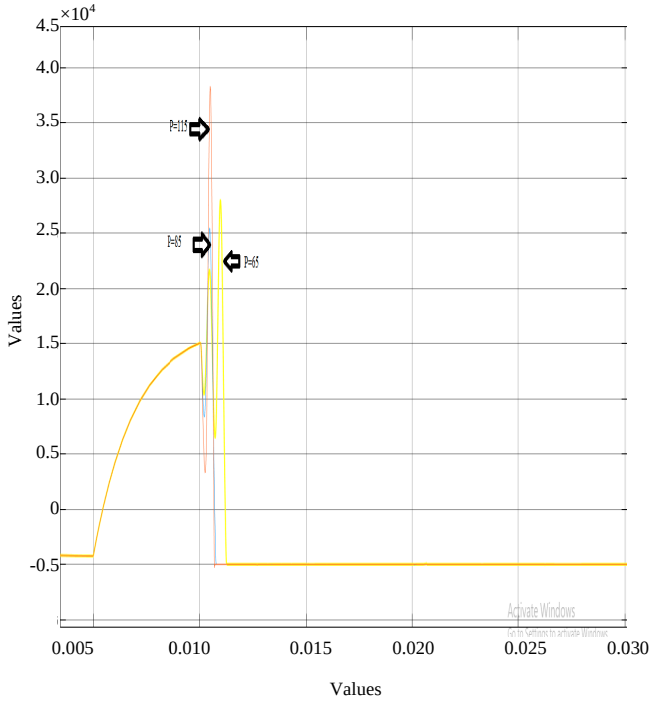


Fig. 18: The current through circuit breaker with various values of P

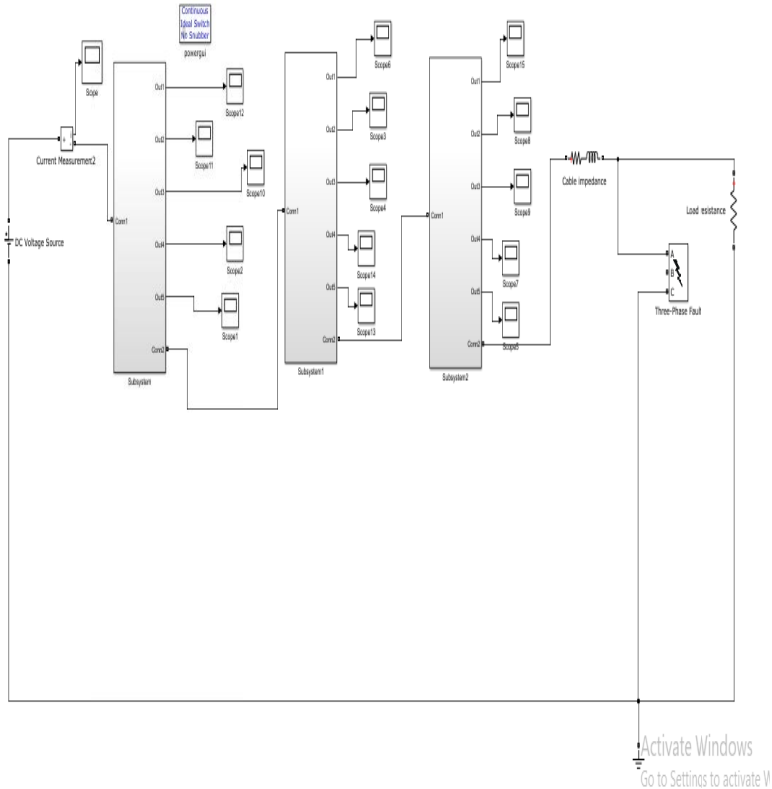


Fig. 19: The model of three series circuit breakers of Mayr model

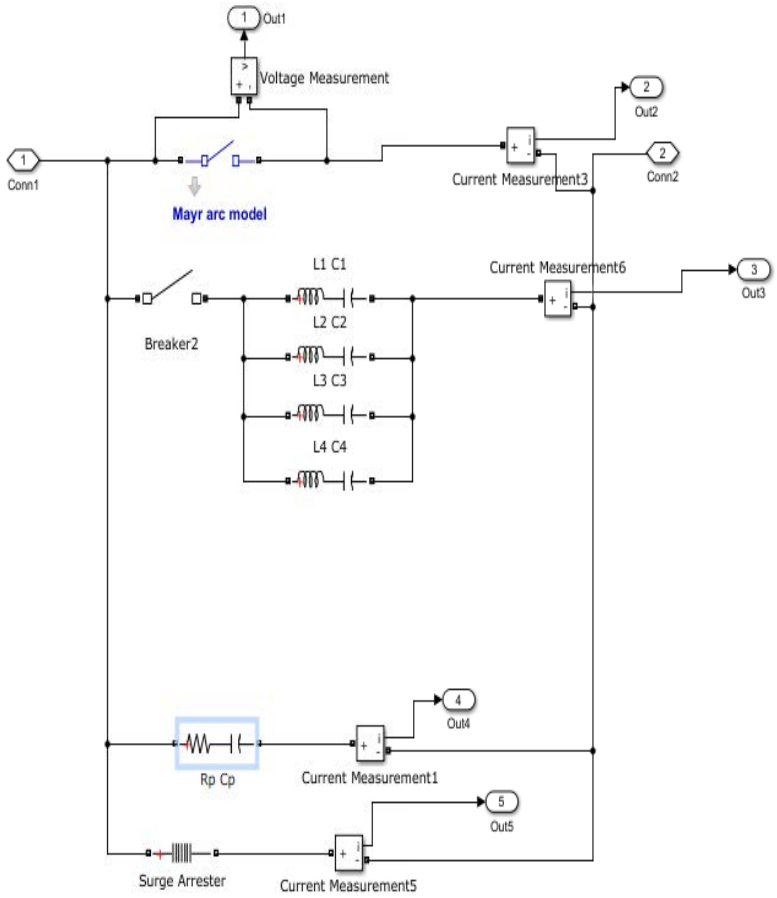


Fig. 20: The subsystem of each circuit breaker of the three series circuit breakers

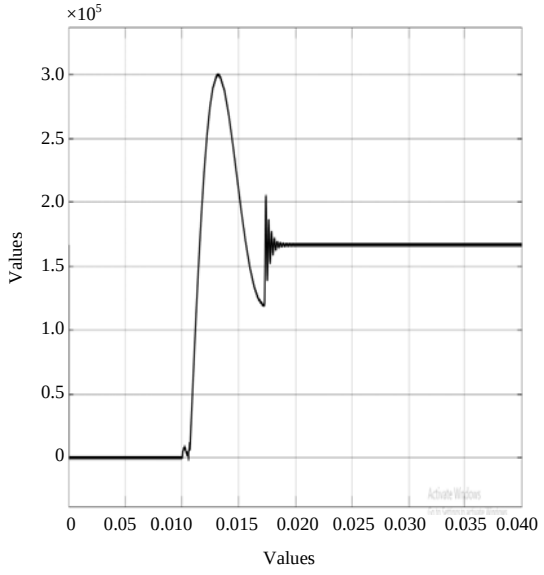


Fig. 21: The voltage across each circuit breaker

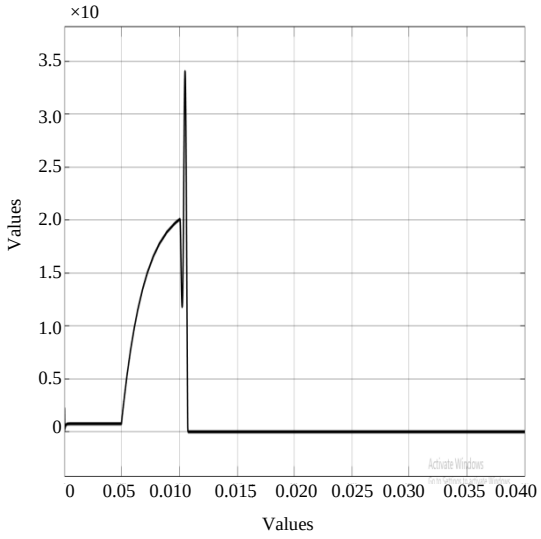


Fig. 22: The current through each circuit breaker

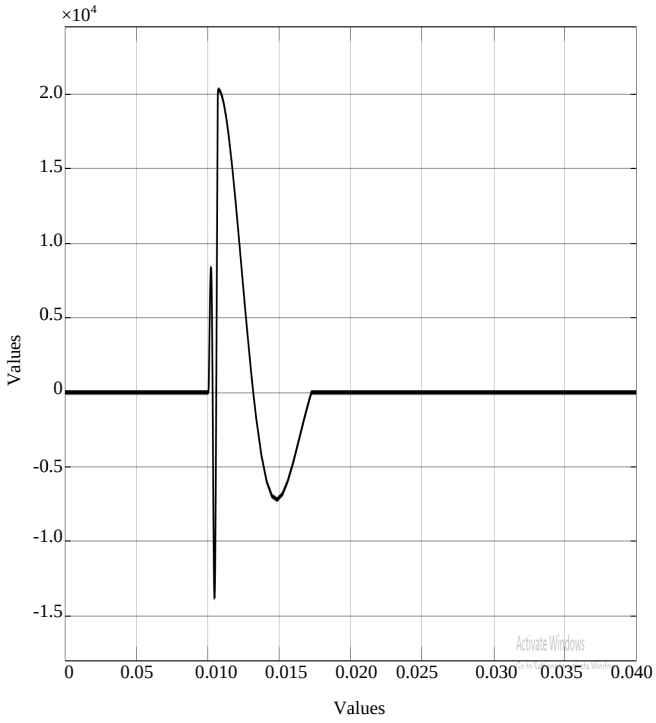


Fig. 23: The current through the commutation circuit in each circuit breaker

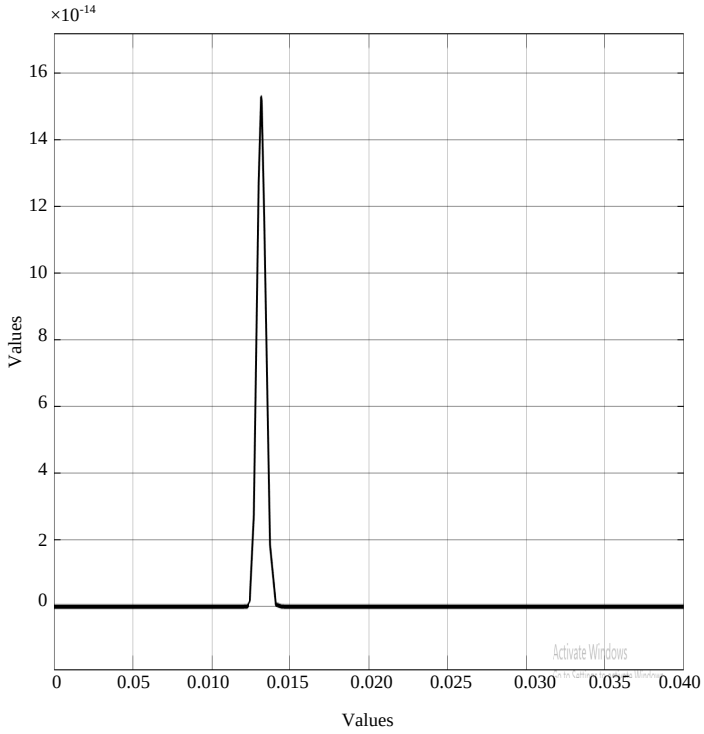


Fig. 24: The current through surge arrester in each circuit breaker

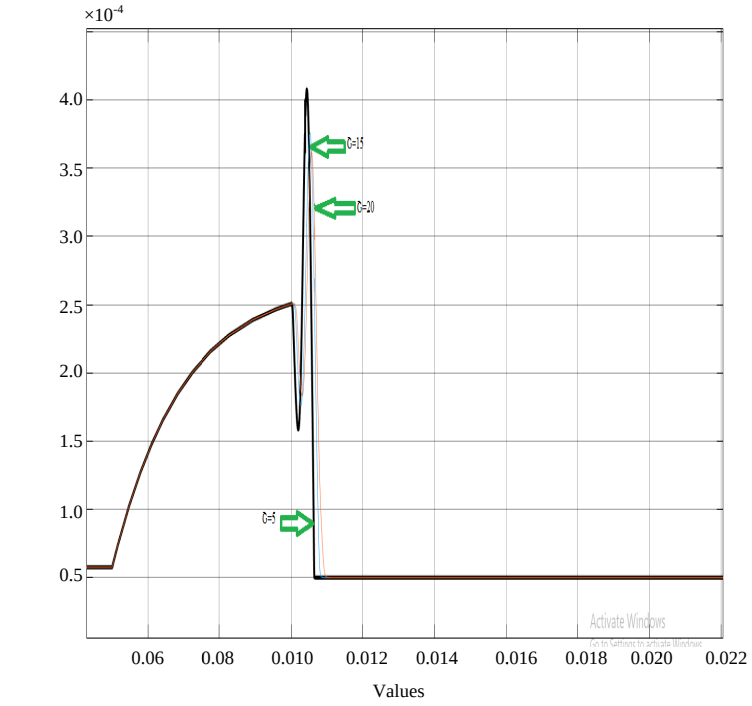


Fig. 25: The current through circuit breaker with various values of ɔ

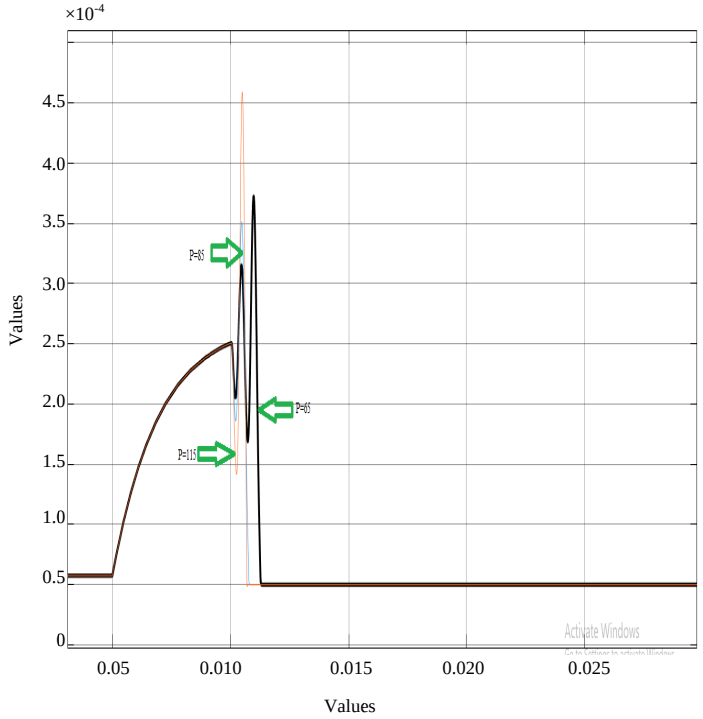


Fig. 26: The current through circuit breaker with various values of P

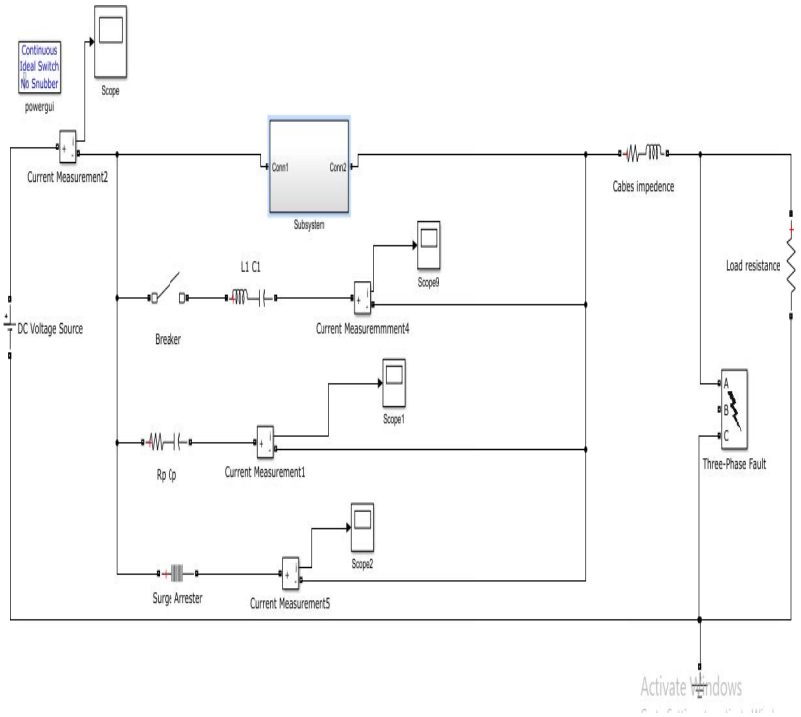


Fig. 27: The main model of circuit breaker consists of three poles

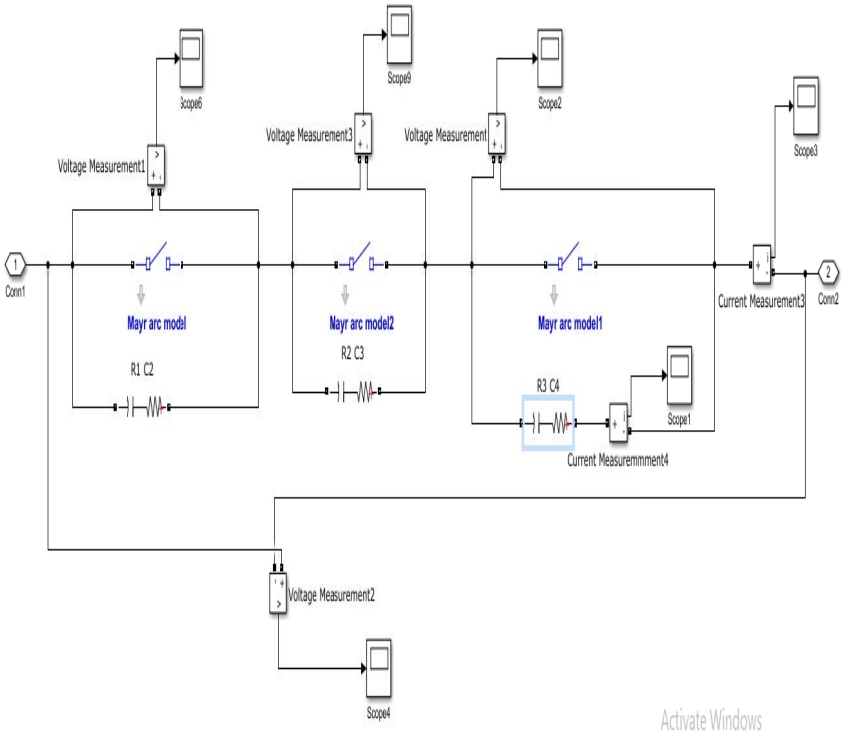


Fig. 28: The subsystem of the circuit breaker

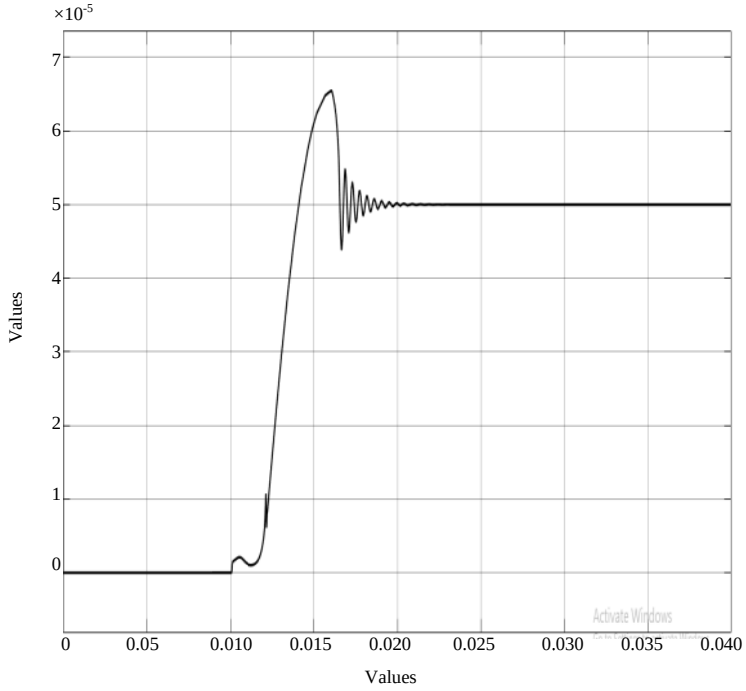


Fig. 29: The total voltage across the circuit breaker

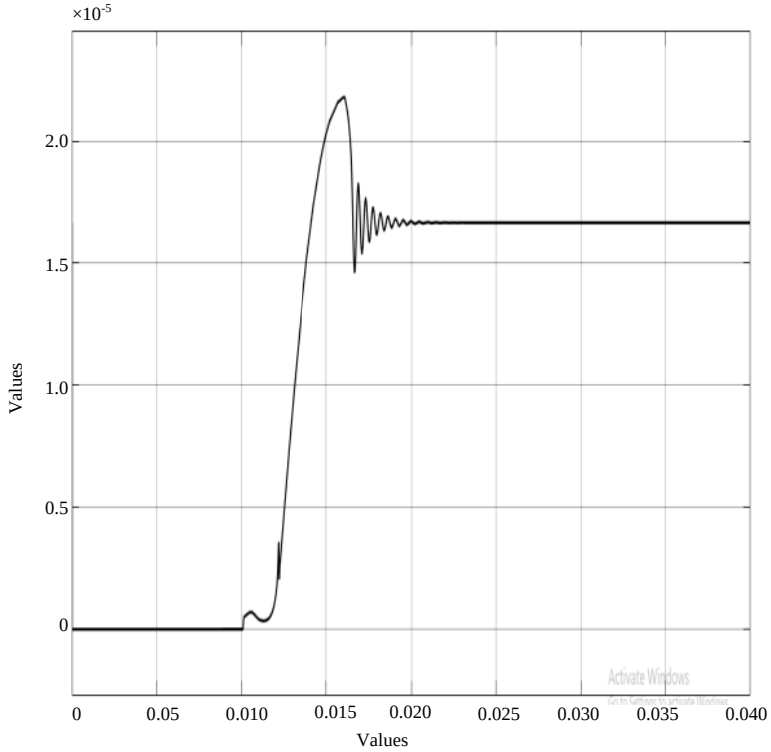


Fig. 30: The voltage across each pole of the circuit breaker

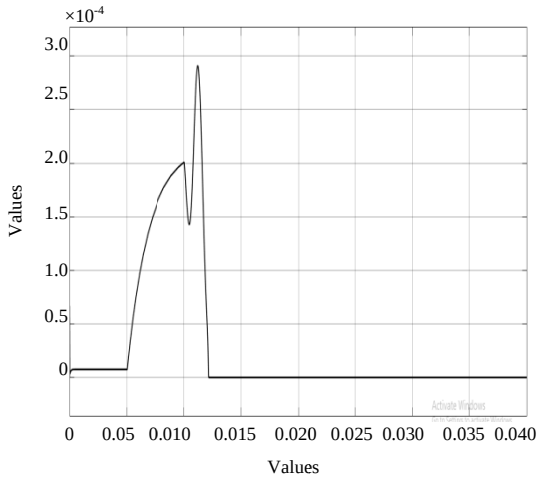


Fig. 31: The current through the circuit breaker

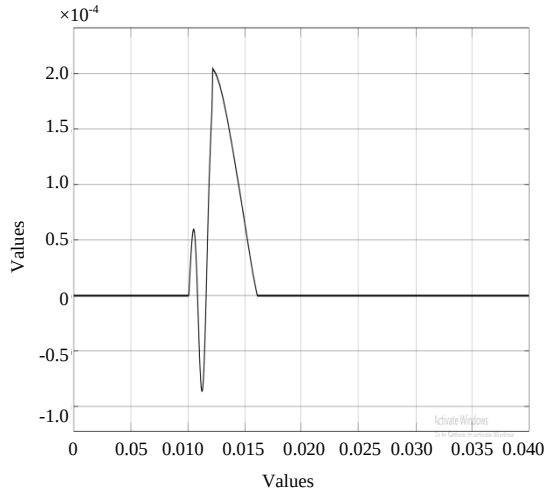


Fig. 32: The current through the commutation circuit

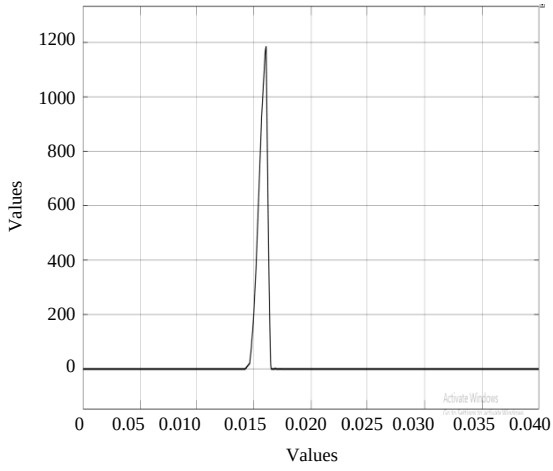


Fig. 33: The current through surge arrester

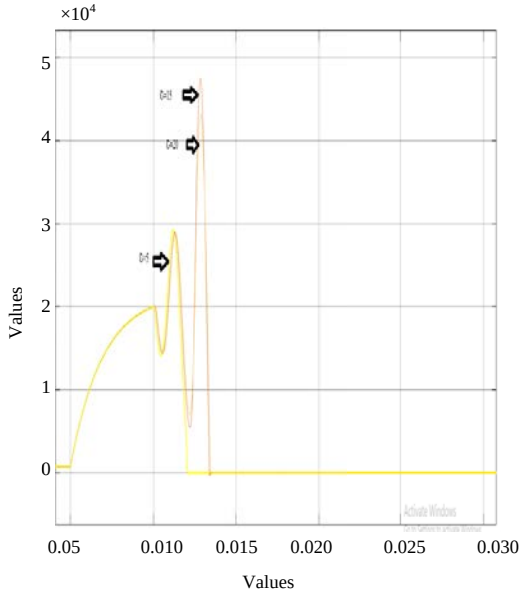


Fig. 34: The current through circuit breaker with various values of ɔ

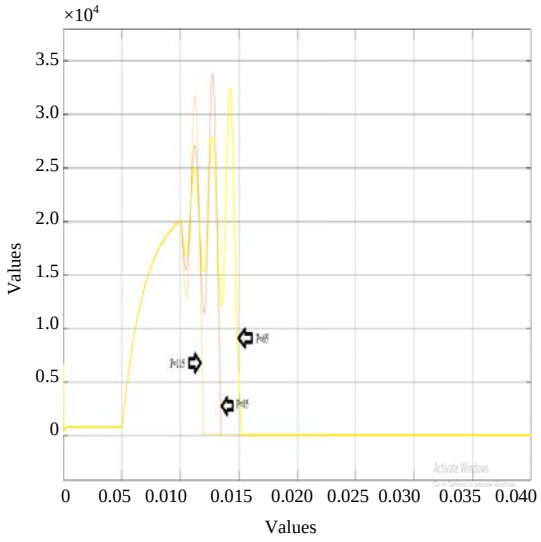


Fig. 35: The current through circuit breaker with various values of P

Table 4: Simulation parameters of the models of Mayr after using three series poles of each circuit breaker

| Model | Parameters | Default values | Tested values |
|---|---|---|---|
| Mayr | P (MW) | 100 | 65, 85, 115 |
| | ɔ (µs) | 10 | 5, 15, 20 |
| | L1 (mH) | 0.25 | 0.25 |
| | C1(µF) | 20 | 20 |
| | Rp (Ω) | 75 | 75 |
| | Cp (µF) | 0.1 | 0.1 |
| | R1, R2 (Ω) | 5 | 5 |
| | C5, C4 (pF) | 100 | 100 |

modification model is greater than the past one. Note that the max peak of voltage across the CB is 654 kV. Figure 34 and 35 illustrate the results of changing the values of P and .

## CONCLUSION

In this study, black box arc model is used to represent the non-linear arc conductance depending on Mayr model. Mayr's model has proved more flexibility to study the effect of different controlled and uncontrolled parameters on the arcing time of HVDC circuit breakers. It is found that the arcing time is reduced by increasing the value of cooling power coefficient, decreasing the arcing time constant, increasing the value of commutation capacitance and decreasing the value of commutation inductance[16]. It is also concluded that using multi-break circuit breaker is better than using number of cascaded series circuit breakers.

## REFERENCES


01. Franck, C.M., 2011. HVDC circuit breakers: A review identifying future research needs. IEEE. Trans. Power Delivery, 26: 998-1007.
02. Meah, K. and S. Ula, 2007. Comparative evaluation of HVDC and HVAC transmission systems. Proceedings of the 2007 IEEE Power Engineering Society General Meeting, June 24-28, 2007, IEEE, Tampa, Florida, pp: 1-5.
03. Mobarrez, M., M.G. Kashani, S. Bhattacharya and R. Adapa, 2014. Comparative study of DC circuit breakers using realtime simulations. Proceedings of the IECON 2014-40th Annual Conference of the IEEE Industrial Electronics Society, October 29-November 1, 2014, IEEE, Dallas, Texas, pp: 3736-3742.
04. Lu, W. and B.T. Ooi, 2003. Optimal acquisition and aggregation of offshore wind power by multiterminal voltage-source HVDC. IEEE. Trans. Power Delivery, 18: 201-206.
05. Meyer, C., M. Hoing, A. Peterson and D.R.W. Doncker, 2007. Control and design of DC grids for offshore wind farms. IEEE. Trans. Ind. Appl., 43: 1475-1482.
06. Anonymous, 2006. Trans-mediterranean interconnection for concentrating solar power. DLR, German Aerospace Center, Institute of Technical Thermodynamics, Section Systems Analysis and Technology Assessment, Germany.
07. Billon, V.C., J.P. Taisne, V. Arcidiacono and F. Mazzoldi, 1989. The Corsican tapping: From design to commissioning tests of the third terminal of the Sardinia-Corsica-Italy HVDC. IEEE. Trans. Power Delivery, 4: 794-799.
08. Kirby, N., L. Xu, M. Luckett and W. Siepmann, 2002. HVDC transmission for large offshore wind farms. Power Eng. J., 16: 135-141.
09. McCallum, D., G. Moreau, J. Primeau, M. Bahrman, B. Ekehov and D. Soulier, 1994. Multi-terminal integration of the Nicolet converter station in to the Quebec-New England phase II HVDC transmission system. Proceedings of the CIGRE 35th International Conference on Large High Voltage Electric Systems, September 1994, Paris, France, pp: 1-9.
10. Greenwood, A., K. Kanngiessner, V. Lesclae, T. Margaard and W. Schultz, 1996. Circuit breakers for meshed multi-terminal HVDC systems. Part II: Switching of transmission lines in meshed MTDC systems. Electra, 164: 62-82.
11. Li, Y., Z. Zhang, C. Rehtanz, L. Luo, S. Ruberg and F. Liu, 2010. Study on steady-and transient-state characteristics of a new HVDC transmission system based on an inductive filtering method. IEEE. Trans. Power Electron., 26: 1976-1986.
12. Guo, C., W. Liu and C. Zhao, 2013. Research on the control method for voltage-current source hybrid-HVDC system. Sci. China Technol. Sci., 56: 2771-2777.
13. Zhang, X., J. Bai, G. Cao and C. Chen, 2013. Optimizing HVDC control parameters in multi-infeed HVDC system based on electromagnetic transient analysis. Int. J. Electr. Power Energy Syst., 49: 449-454.
14. Chang, B., O. Cwikowski, M. Barnes and R. Shuttleworth, 2015. Multi-terminal VSC-HVDC pole-to-pole fault analysis and fault recovery study. Proceedings of the 11th IET International Conference on AC and DC Power Transmission, February 10-12, 2015, Birmingham, UK., pp: 1-8.
15. Mohammadi, M., M. Avendano-Mora, M. Barnes and J.Y. Chan, 2013. A study on fault ride-through of VSC-connected offshore wind farms. Proceedings of the 2013 IEEE Power & Energy Society General Meeting, July 21-25, 2013, IEEE, Vancouver, Canada, pp: 1-5.
16. Gouda, O.E., D.K. Ibrahim and A. Soliman, 2018. Parameters affecting the arcing time of HVDC circuit breakers using black box arc model. IET. Gener. Transm. Distrib., 13: 461-467.
17. Xiang, B., L. Zhang, K. Yang, Y. Tan and Z. Liu *et al*., 2016. Arcing time of a DC circuit breaker based on a superconducting current-limiting technology. IEEE. Trans. Applied Supercond., 26: 1-5.
18. May, T.W., Y.M. Yeap and A. Ukil, 2016. Comparative evaluation of power loss in HVAC and HVDC transmission systems. Proceedings of the 2016 IEEE Region 10 Conference (TENCON), November 22-25, 2016, IEEE, Singapore, pp: 637-641.

19. Darwish, H.A., M.A. Izzularab and N.I. Elkalashy, 2006. Enhanced commutation circuit design of HVDC circuit breaker using EMTP. Proceedings of the 2005/2006 IEEE/PES Transmission and Distribution Conference and Exhibition, May 21-24, 2006, IEEE, Dallas, Texas, pp: 978-985.
20. Qin, T., E. Dong, G. Liu and J. Zou, 2016. Recovery of dielectric strength after DC interruption in vacuum. IEEE. Trans. Dielectr. Electr. Insul., 23: 29-34.
21. Lim, S.W., U.A. Khan, J.G. Lee, B.W. Lee, K.S. Kim and C.W. Gu, 2015. Simulation analysis of DC arc in circuit breaker applying with conventional black box arc model. Proceedings of the 2015 3rd International Conference on Electric Power Equipment-Switching Technology (ICEPE-ST), October 25-28, 2015, IEEE, Busan, South Korea, pp: 332-336.
22. Nakao, H., Y. Nakagoshi, M. Hatano, T. Koshizuka and S. Nishiwaki *et al*., 2001. Dc current interruption in HVDC SF6 gas MRTB by means of self-excitation. IEEE. Power Eng. Rev., 21: 62-62.
23. Smeets, R.P.P. and V. Kertesz, 2013. Application of a validated AC black-box arc model to DC current interruption. Proceedings of the 2013 2nd International Conference on Electric Power Equipment-Switching Technology (ICEPE-ST), October 20-23, 2013, IEEE, Matsue, Japan, pp: 1-4.
24. Zhu, K., X. Li, S. Jia, W. Zhang and W. Gao, 2015. Study of the switching arc characteristics of a 500 kV HVDC self-excited oscillatory metallic return transfer breaker. IEEE. Trans. Dielectr. Electr. Insul., 22: 128-134.
25. Walter, M. and C. Franck, 2014. Improved method for direct black-box arc parameter determination and model validation. IEEE. Trans. Power Delivery, 29: 580-588.
26. Pauli, B., G. Mauthe, E. Ruoss and G. Ecklin, 1988. Development of a high current HVDC circuit breaker with fast fault clearing capability. IEEE. Trans. Power Delivery, 3: 2072-2080.
27. Greenwood, A., K. Kanngiessner, V. Lesclae, T. Margaard and W. Schultz, 1995. Circuit breakers for meshed multi-terminal HVDC systems part I: Introduction DC side substation switching under normal and fault conditions. Electra, 163: 98-122.
28. Garzon, R.D., 2002. High Voltage Circuit Breakers High Voltage Circuit Breakers: Design and Applications. 2nd Edn., Marcel Dekker Publishing, New York, USA.,.
29. De Andrade, V. and E. Sorrentino, 2010. Typical expected values of the fault resistance in power systems. Proceedings of the 2010 IEEE/PES Transmission and Distribution Conference and Exposition: Latin America (T&D-LA), November 8-10, 2010, IEEE, Sao Paulo, Brazil, pp: 602-609.
30. Ohtaka, T., V. Kertesz and R.P.P. Smeets, 2017. Novel black-box arc model validated by high-voltage circuit breaker testing. IEEE. Trans. Power Delivery, 33: 1835-1844.
31. Esenwein, F.D. and R.G. Colclaser, 1995. Simulation of arc-circuit instability in a low current DC automotive switching application. IEEE. Trans. Veh. Technol., 44: 348-355.
32. Pugliese, H. and M. Vonkannewurff, 2010. Direct current circuit breaker primer. Proceedings of the 2010 Record of Conference Papers Industry Applications Society 57th Annual Petroleum and Chemical Industry Conference (PCIC), September 20-22, 2010, IEEE, San Antonio, Texas, pp: 1-7.
33. Lee, J.G., U.A. Khan, H.Y. Lee and B.W. Lee, 2016. Impact of SFCL on the four types of HVDC circuit breakers by simulation. IEEE. Trans. Applied Supercond., 26: 1-6.
34. Bizzarri, F., A. Brambilla, G. Gruosso, G.S. Gajani, M. Bonaconsa and F. Viaro, 2017. A new black-box model of SF 6 breaker for medium voltage applications. Proceedings of the IECON 2017-43rd Annual Conference on IEEE Industrial Electronics Society, October 29-November 1, 2017, IEEE, Beijing, China, pp: 32-37.
35. Park, K.H., H.Y. Lee, M. Asif, B.W. Lee, T.Y. Shin and C.W. Gu, 2017. Assessment of various kinds of AC black-box arc models for DC circuit breaker. Proceedings of the 2017 4th International Conference on Electric Power Equipment-Switching Technology (ICEPE-ST), October 22-25, 2017, IEEE, Xi'an, China, pp: 465-469.